

S15

HIGH TEMPERATURE X-RAY POWDER DIFFRACTION AS A TOOL FOR MONITORING OF THERMALLY INDUCED TRANSFORMATION OF γ - Fe_2O_3 IN VARIOUS ATMOSPHERES

J. Kašlík, O. Malina, I. Medřík, J. Filip, R. Zbořil

*Regional Centre of Advanced technologies and Materials, Departments of Experimental Physics and Physical Chemistry, Faculty of Science, Palacký University Olomouc, 17. listopadu 1192/12, 771 46 Olomouc, Czech Republic
josef.kaslik@upol.cz*

Iron oxide nanomaterials became one of the most studied materials up to date due to their significantly different properties comparing to their bulk counterparts. Generally, four crystalline form of iron(III) oxide exist exhibiting different crystallographic and magnetic properties. We present thermally induced solid state transformations of one of the rare iron(III) oxide polymorph, i.e., γ - Fe_2O_3 , by view of high temperature X-ray powder diffraction. All transformation experiments were performed in very similar conditions (i.e., temperature increment, gas pressure) with only difference in exchange of reaction gases. Gases were chosen to represent oxidative, inert, and reductive atmospheres (i.e., synthetic air, CO_2 , N_2 , H_2). Transformation in the oxidative atmosphere of synthetic air led directly to creation of the most stable iron(III) oxide polymorph, i.e., hematite, in temperature range 680 – 760 °C. Transformation per-

formed in carbon dioxide atmosphere led to creation of magnetite via hematite at temperature range 475 – 700 °C. Transformation scheme of experiment performed in nitrogen atmosphere, which is considered as inert, was more complicated and transformation via two intermediates (i.e., hematite and magnetite) led to final product identified as wustite, which was created between 800 and 900 °C. In these experiments, all intermediates and final products were investigated at room temperature by view of X-ray powder diffraction and Mössbauer spectroscopy to confirm the phase composition and iron ions state. Reductive atmosphere of hydrogen led to creation of metallic iron as expected due to the nature of reducing gas.

The authors gratefully acknowledge the financial support by Internal IGA grant of Palacký University Olomouc, Czech Republic (IGA_PrF_2015_017).

S16

STUDIA STRUKTURY HEUSLEROVÝCH SLITIN POMOCÍ RENTGENOVÝCH METOD

Petr Cejpek¹, Václav Holý¹, Jan Endres¹, Oleg Heczko², Lukáš Horák¹

¹Katedra fyziky kondenzovaných látek, Matematicko-fyzikální fakulta UK, Ke Karlovu 5, 121 16 Praha 2

²Fyzikální ústav AV ČR, v. v. i., Na Slovance 1999/2, 182 21 Praha 8

petr.cejpek@centrum.cz

Heuslerovy slitiny jsou v poslední době studovány pro svou škálu zajímavých vlastností – a už magnetických či elektronických. Tyto vlastnosti podstatně závisí na krystalové struktuře. Jako zástupci pro studium struktury byly zvoleny série vzorků $\text{Mn}_2\text{Co}_{1-x}\text{Rh}_x\text{Sn}$ a slitina Ni_2MnGa .

První jmenovaná sloučenina byla studována pomocí práškové difrakce na čarách CoK a CuK a metodou EXAFS. Z práškové difrakce vyplývá, že struktura prochází tetragonální distorzí přibližně okolo $x = 0.3$ obsahu Rh. V Heuslerových slitinách se může vyskytovat několik typů okupačního nepořádku (popsané například v [1]). Některé z nich se dají vyloučit díky absenci specifických difrakcí v práškovém záznamu. Nepořádek byl studován fitováním integrálních intenzit z práškových záznamů a fitování EXAFSových dat změřených na absorpční hraně CoK a MnK. EXAFS ukazuje, že uvažování okupačního nepořádku je nezbytné ke správnému zpracování dat. Fit bez nepořádku totiž vede k velké kontrakci mřížových parametrů, což není fyzikálně možné

(prášková difrakce byla znovu změřena po EXAFSovém měření a mřížové parametry se nemění).

Druhý vzorek, Ni_2MnGa , je členem slitin s tvarovou pamětí a jeho struktura může být dobře modifikována drobnými změnami v kompozici. Doposud byla struktura Ni_2MnGa studována většinou práškovou difrakcí [2], naše studie naproti tomu probíhaly na monokrystalickém vzorku. Složení našeho vzorku bylo určeno pomocí EDX jako $\text{Ni}_{50.1}\text{Mn}_{28.4}\text{Ga}_{21.5}$. Z měření vyplývá že základní struktura našeho vzorku je monoklinní, která se však nepříliš liší od tetragonální. Ví se [3], že Ni_2MnGa může vytvářet dvojčatovou strukturu. Přítomnost dvojčatových domén byla potvrzena monokrystalickou difrakcí. Z výsledků vyplývá, že ve vzorku existuje modulovaná 10M struktura, protože se v záznamu objevila satelitní maxima, kterým jsme přiřadili neceločíselné indexy. Tato modulace může být popsána harmonickou vlnou, jejíž koeficienty jsme získali fitováním integrálních intenzit. Na vzorku byla rovněž změřena difrakce za vysokých teplot. Přechod do vysokoteplotní austenitické fáze vykazuje



hysterezi – k přechodu došlo při 62 °C při o hřevu a při 50 °C při chlazení.

1. T. Graf, et al., *Simple rules for the understanding of Heusler compounds*, Progress in Solid State Chemistry 39(1):1-50, 2011, DOI: <http://dx.doi.org/10.1016/j.progsolidstchem.2011.02.001>.

2. S.Singh et al., *High-resolution synchrotron x-ray powder diffraction study of the incommensurate modulation in the martensite phase of Ni₂MnGa*, PRB 90(1):014109, 2014, DOI: [10.1103/PhysRevB.90.014109](https://doi.org/10.1103/PhysRevB.90.014109).
3. Ge Yanling, *The Crystal and Magnetic Microstructure of Ni-Mn-Ga alloys*, Doctoral thesis, Espoo, 2007.

S17

ACCURACY OF STRUCTURE ANALYSIS OF SINGLE NANOCRYSTALS BY PEDT

C. A. Correia^{1,2}, L. Palatinus¹, M. Klementová¹

¹Department of Structure Analysis, AS CR, Cukrovarnická 10/112, Prague- Czech Republic

²Department of Physics of Materials, Charles University Prague, Ke Karlovu 5, Prague – Czech Republic
cinthiacac@gmail.com

The development and improvement of nanomaterials require the accurate structure analysis of single nanocrystals. Electron diffraction (ED) allows the structure analysis of single nanocrystals as small as tens of nanometers thanks to the strong interaction between electrons and matter, compared to X-rays, and has already been used for some time for this purpose [1-4]. The three-dimensional information of the reciprocal space may be obtained by using electron diffraction tomography (EDT) [5,6], which consists of tilting the crystal in small steps around the axis of the goniometer and collecting a diffraction pattern at each position. Because the angular position between the patterns is known, the three-dimensional information of the reciprocal space can be reconstructed. However, multiple scattering of the beam cannot be neglected for ED. One remedy to these dynamical interactions is to use precession electron diffraction (PED) [7, 8], where the beam is precessed around the optical axis of the microscope, making a cone surface with the vertex at the sample. The beam is deflected back to the optical axis after passing through the sample, resulting in reflection spots in the pattern (Fig. 1). PED data sets have the intensities integrated over all the positions of the beam during the precession, resulting in intensities less sensitive to multiple scattering effects and crystal defects and more sensitive to structure parameters. Several structures of nanocrystalline materials of diverse complexity have been determined using precession electron diffraction tomography (PEDT) [9-11]. Despite of giving reliable structure solution, the use of kinematical approximation is not suitable for the least-squares structure refinement against ED data. Such refinement results in higher figures of merit and lower accuracy of structure parameters. To properly account for the dynamical character of electron diffraction, the dynamical theory of diffraction should be used. The usefulness of the dynamical refinement for PEDT data was recently demonstrated [12, 13] and it was shown to give more accurate structure parameters and lower figures of merit when compared to refinements using the kinematical approximation. In this work, the comparison of the kinematical and the dynamical refinements with the reference structure obtained by single crystal X-ray diffraction is presented for 5 samples. The comparison is performed between the standard crystallographic residue parameters $R1(\text{obs})$, $wR(\text{all})$, average distance from the

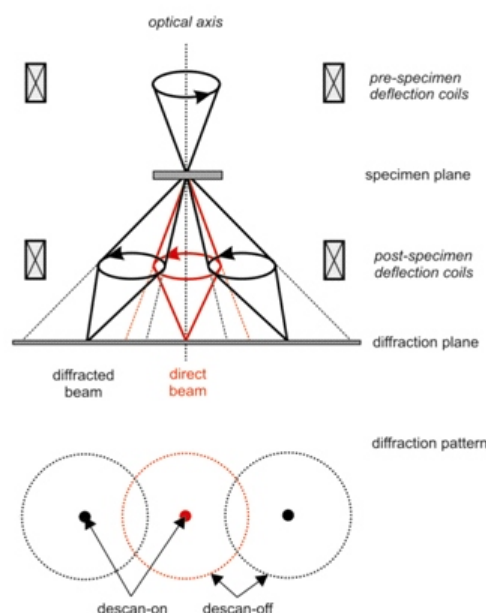


Figure 1. During the precession electron diffraction, the beam is deflected from the optical axis of the microscope, making a cone surface with the vertex at the sample. The post-specimen coils deflect the beam back, resulting in a diffraction pattern with spots instead of circles.

reference atomic position (ADRA) and maximal distance from the reference atomic position (MDRA). It is shown that the PEDT model refined using the dynamical theory of diffraction matches very well with the reference structure, with lower figures of merit and an average distance from the reference atom (ADRA) lower than 0.021 Å (Tab. 1).

1. B. K. Vainshtein, *Electron Diffraction Structure Analysis*. New York: Plenum Press. 1964.
2. J. M. Cowley, *Electron Diffraction Techniques*, Vols 1 and 2. Oxford University Press. 1992.
3. D. L. Dorset, *Structural Electron Crystallography*, New York: Plenum Press. 1995.
4. U. Kolb, T. Gorelik, E. Mugnaioli, *Materials Research Society Symposium Proceedings*, 1184, (2009).

Table 1. Samples used in the comparison of the dynamical refinement against the reference structure and the kinematical refinement.

Sample	Ni ₃ Si ₂		Ni ₂ Si		Orthopyroxene		Kaolinite		PrVO ₃	
Tilt angle (°)	-56 56		-25 48		-45 45		-50 50		-56 59	
PED angle (°)	2.0		1.5		2.0		1.0		1.5	
Space group	<i>Cmcm</i>		<i>Pnma</i>		<i>Pbca</i>		<i>C1</i>		<i>Pbnm</i>	
Indepen. atoms	10		3		10		13		4	
Ref	Kin	Dyn	Kin	Dyn	Kin	Dyn	Kin	Dyn	Kin	Dyn
R1(obs)	17.95	8.99	11.07	7.14	24.22	8.33	19.16	6.23	24.04	6.95
wR(all)	21.34	10.78	11.53	7.56	29.44	9.48	20.11	6.54	26.19	6.80
GOF(all)	12.82	2.63	4.38	1.42	17.45	3.38	9.29	2.36	9.86	8.23
Ref/Par	549/28	8034/140	88/10	849/84	876/42	10452/133	1057/52	2377/154	369/11	2741/128
ADRA	0.01634	0.00819	0.02035	0.00826	0.031	0.016	0.097	0.021	0.141	0.016
MDRA	0.04820	0.01935	0.02843	0.01351	0.066	0.033	0.270	0.042	0.239	0.020

- U. Kolb, T. Gorelik, C. Kuebel, M. T. Otten, D. Hubert, *Ultramicroscopy*, 107, (2007), 507.
- U. Kolb, T. Gorelik, M. T. Otten, *Ultramicroscopy*, 108, (2008), 763.
- R. Vincent, P. A. Midgley, *Ultramicroscopy*, 53, (1994), 271.
- E. Mugnaioli, T. Gorelik, U. Kolb, *Ultramicroscopy*, 109, (2009), 758.
- D. Jacob, P. Cordier, *Ultramicroscopy*, 110, (2010), 1166.
- L. Palatinus, M. Klementová, V. Dřinec, M. Jarošová, V. Petříček, *Inorganic Chemistry*, 50, (2011), 3743.
- U. Kolb, E. Mugnaioli, *Microporous and Mesoporous Materials*, 189, (2014), 107.
- L. Palatinus, J. Damien, P. Cuvillier, M. Klementová, W. Shinkler, L. D. Marks, *Acta Crystallographica*, A69, (2013), 171.
- L. Palatinus, V. Petříček, C. A. Correia, *Acta Crystallographica*, A71, (2015), 235.

This project is financially supported by the Czech Science Foundation, project number 13-25747S.

S18

STUDY OF TEMPERATURE STABILITY OF TITANATE NANOTUBES UP TO 800 °C

Tereza Brunatova¹, Alexandra Rudajeva¹, Michal Vaclav², Stanislav Danis¹, Daniela Popelkova³, Radomir Kuzel¹

¹Charles University, Faculty of Mathematics and Physics, Dept. of Condensed Matter Physics, Prague

²Charles University, Faculty of Mathematics and Physics, Dept. of Surface and Plasma Science, Prague

³Institute of Macromolecular Chemistry, Academy of Sciences of the Czech Republic, Prague

Study of temperature stability of titanate nanotubes (Ti-NT) is important because some of possible applications of Ti-NT require heating [1]. By heating of Ti-NT at low temperature range (from room temperature till approximately 200 °C) the releasing of the adsorbed and interlayer water were observed [2-5]. These releasing of water were observed by X-ray diffraction [2, 4] and DSC analysis [3, 5]. At higher temperature the anatase structure of TiO₂ started grow [4, 5]. Finally at the temperature higher than 700 °C the nanotubes transform to nanorods with structure:

Na₂Ti₆O₁₃ [2-5] and nanoparticles with rutile structure of TiO₂ [4-5].

In this contribution, the structure changes of titanate nanotubes will be studied by combination of powder X-ray diffraction, differential scanning calorimetry, thermal gravimetric analysis and mass spectroscopy. The study was done in two atmosphere - air and inert atmosphere (vacuum, helium). In air and inert atmosphere, the releasing of water was observed by X-ray diffraction, DSC and confirm with mass spectroscopy at low temperature. The transformation to anatase structure of TiO₂ was observed by pow-



der X-ray diffraction and DSC in air and inert atmosphere. However other transformation at high temperature to $\text{Na}_2\text{Ti}_6\text{O}_{13}$ and rutile structure of TiO_2 was observed only in air atmosphere. In vacuum atmosphere the anatase was only stable phase. In He the black rutile was found on DSC curve.

1. Bavykin DF. V., Walsh F. C.: Titanate and titania nanotubes, synthesis, properties and application, RSC Publishing, 2010.
2. Nikolic L. M., Maletin M., Ferreira P., and Vilarinho P. M.: Synthesis and characterization of one-dimensional titanate structure. Processing and application of ceramics, 2, 2008.

3. Yu D.-N., Liu W.-X., Ma J., Qu X.-G., Cao W.-B., Zhang Z./Y., and Mao J.-H.: Preparation of titanate nanotubes by hydrotherm method. *Material Science Forum*, 620-622, 2009.
4. Yoshida R., Suzuki Y., and Yoshikawa S.: Effects of synthetic conditions and heat-treatment on the structure of partially ion-exchange titanate nanotube. *Materials chemistry and physics*, 91, 2005.
5. Morgado E., jr, de Abreu M. A. S., Pravia O. R. C., Marinkovic B. A., Jardim P. M., rizzo R.C., Araujo A.S.: A study on the structure and thermal stability of titanate nanotubes as a function of sodium content, *Solid State Science*, 8, 2006.

S19

STUDY OF PARTICLE GROWTH IN TITANIUM ALLOYS USING X-RAY DIFFRACTION

Jana Šmilauerová, Václav Holý, Zdeněk Matěj, Jiří Pospíšil

Faculty of Mathematics and Physics, Charles University in Prague, Ke Karlovu 5, Praha 2, 121 16
jana.smilauerova@gmail.com

Metastable titanium alloys exhibit unique mechanical and functional properties, such as high specific strength, excellent corrosion resistance and good biocompatibility [1]. Therefore, metastable titanium alloys are prospective materials for a number of application fields, including automobile and aircraft industry or biomedical devices. Metastable titanium alloys contain a sufficient amount of -stabilizing elements to retain the high temperature phase (body-centred cubic) in a metastable state upon rapid cooling to room temperature. However, the thermodynamically stable composition consists of a mixture of the phase and particles of the low temperature phase (hexagonal close-packed) [2]. Phase transformations occurring in these alloys are very complex, as several additional metastable phases can form. One of the most intriguing of these phases is the phase which occurs as nanoparticles of hexagonal structure homogeneously distributed throughout the matrix. These particles display an ellipsoidal morphology and are coherent with the matrix. The particles form by a diffusionless displacive transformation from the parent phase [3] and upon ageing at elevated temperatures further evolve by a diffusion-driven process [4]. The exact mechanisms of particle formation and growth are still neither satisfactorily described, nor fully understood.

This research was conducted on TIMETAL LCB (Ti-6.8Mo-4.5Fe-1.5Al in wt.%) metastable titanium alloy. For the purpose of this study, single-crystals of this alloy were grown in an optical floating zone furnace [5]. The resulting single-crystals were solution treated above the -transus temperature and quenched to water. Subsequently, different conditions were prepared from this material by ageing at 300 °C for 8 h, 16 h, 32 h, 64 h, 128 h and 256 h. Then we measured coplanar reciprocal space maps around the $\{1\bar{1}2\}$ maximum of the phase and around the

$\{112\}$ maximum of the matrix in all the samples, see Fig. 1 and Fig. 2, respectively. The

maxima exhibited an ellipsoidal shape which was fitted using a model of diffusely scattered intensity. The shape of $\{112\}$ peaks substantially differ from the maxima, as it is affected by diffuse scattering from particles and other defects in the structure. From the fit of the shape of peaks, the mean particle sizes along its c -axis (denoted by R_c) as well as along its a -axis (R_a) were calculated, see Fig. 3. It was found out that the size of the aged parti-

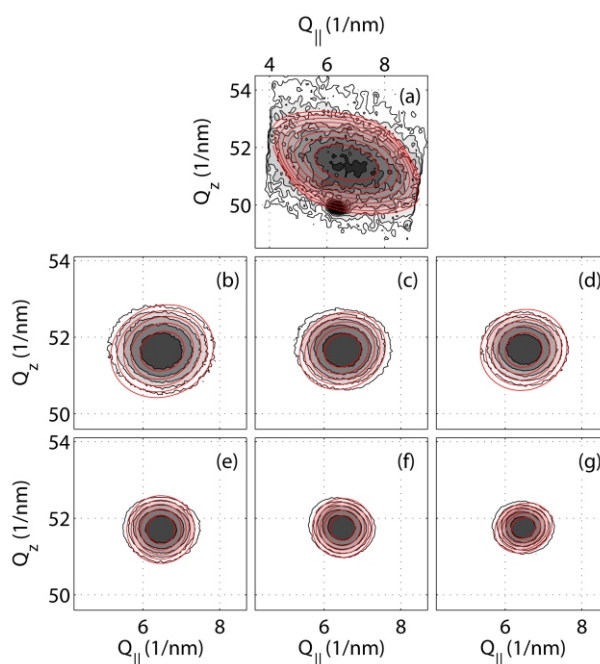


Figure 1. Coplanar reciprocal space maps measured in the maximum $\{1\bar{1}2\}$ of the phase particles. Solution treated sample (a) and samples after ageing for 8 – 256 h (b – g). The red lines in the left panel represent simulated intensity distributions.

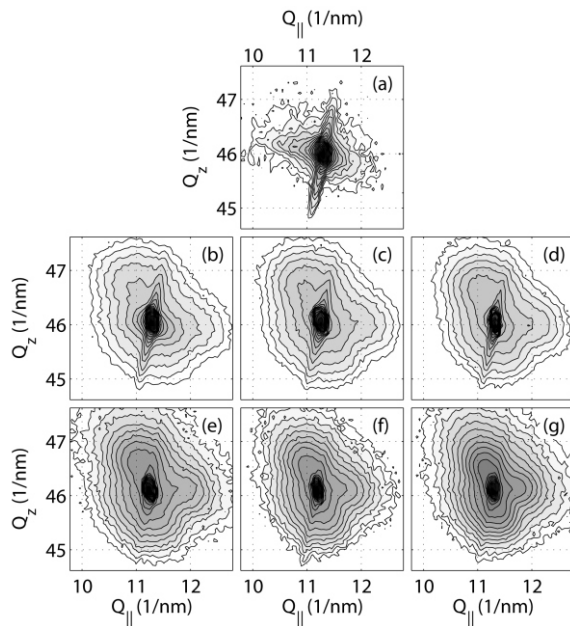


Figure 2. Coplanar reciprocal space maps measured in the $\{112\}$ maximum of the matrix. Solution treated sample (a) and samples after ageing for 8 – 256 h (b - g).

cles is almost spherical and that the radius obeys a dependence $t^{1/3}$, where t is the ageing time. This dependence was observed also for a number of other systems and is known as the Lifshitz, Slyozov and Wagner model [6]. This law holds for diffusion-controlled growth of particles under the influence of precipitate-matrix interface energy. The components of the misfit of the lattice with respect to the lattice of the matrix were also determined, see Fig. 4. The largest misfit is observed in the solution treated sample. With increasing ageing time, the misfit is decreasing. This effect is most likely caused by an outward diffusion of alloying elements from the volume of the particles which accompanies the growth of the phase particles.

1. P. J. Bania, *JOM Journal of the Minerals, Metals and Materials Society*, **46**, (1994), 16 - 19.
2. G. Lütjering and J. C. Williams, *Titanium*, Berlin: Springer, 2003.
3. D. De Fontaine, *Acta Metallurgica*, **18**, (1970), 275 - 279.

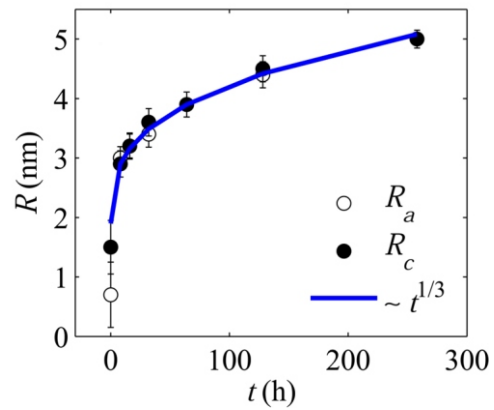


Figure 3. The dependence of the particle radii on the ageing time.

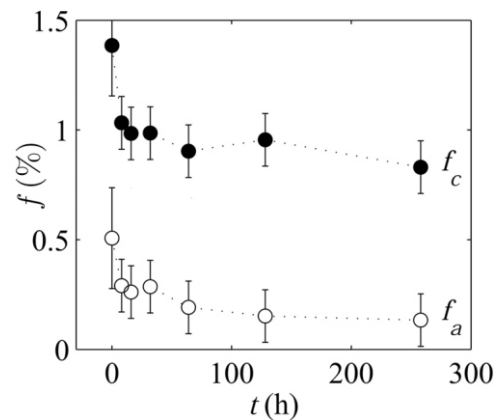


Figure 4. The dependence of the misfit components along the two main axes of the hexagonal lattice on the ageing time.

4. A. Devaraj, R. E. A. Williams, S. Nag, R. Srinivasan, H. L. Fraser and R. Banerjee, *Scripta Materialia*, **61**, (2009), 701 – 704.
5. J. Šmilauerová, J. Pospíšil, P. Harcuba, V. Holý and M. Janěček, *Journal of Crystal Growth*, **405**, (2014), 92 - 96.
6. M. Lifshitz and V. V. Slyozov, *Journal of Physics and Chemistry of Solids*, **19**, (1961), 35–50.